Evaluation of Raman microscopy for the detection of additional monosodium glutamate in dry soup mix

N. Çebi[1], T. Öztürk[2], C.E. Doğan[2] and O. Sağdıç[1]

[1]Food Engineering Department, Chemical and Metallurgical Engineering Faculty, Yıldız Technical University, 34210, İstanbul, Turkey; [2]Food Institute, TUBITAK MRC, 41470 Gebze-Kocaeli, Turkey

Corresponding Authors: N. Çebi, nurcebi@yildiz.edu.tr; C.E. Doğan, canan.dogan@tubitak.gov.tr

Received: 20 January 2019 / Accepted: 11 November 2019 / Published: 6 January 2020

RESEARCH ARTICLE

Abstract

This article presents Raman chemical mapping application for the detection of adulterant monosodium glutamate (MSG) in dry soup mix. MSG may cause various damages to the health of people. Therefore, there are legal regulations for this compound both in Turkish Food Codex and European Union Directives. Most of the times, the main problem is that MSG is added into dry soup products without declaration on the label. Food control mechanisms need effective and real-time monitoring methods to check the reliability of the product labels in order to maintain food safety and alleviate public doubts. In this study, MSG was added into dry soup mix at a concentration (w/w) of 0.1, 0.2, 0.4 and 0.6% and chemical maps were obtained using multivariate data analysis techniques such as direct classical least squares (DCLS) component analysis. MSG was successfully detected and spectral and spatial distribution of the MSG within the commercial and laboratory-prepared dry soup samples was accomplished, with a detection limit of 0.1%. The results obtained were confirmed by a robust liquid chromatography-tandem mass spectrometry (LC-MS/MS) technique.

Keywords: monosodium glutamate, Raman, mapping, imaging, DCLS

1. Introduction

Glutamic acid has been known as a widespread amino acid present in foodstuffs. L-configuration of glutamic acid is used as a flavour enhancer globally (Populin *et al.*, 2007). Generally, commercial amino acids are obtained by using four well-known methods: extraction from natural sources, chemical synthesis, fermentation and enzymatic catalysis. It is possible to obtain glutamic acid by isolation from numerous sources, such as wheat gluten, soybean meal and casein (Ault, 2004). Monosodium glutamate (MSG), the sodium salt of glutamic acid, has been used worldwide as a food additive or seasoning to enhance the flavour of various foods. MSG enhances the 'sixth flavour' (*umami*), which means 'savoury' or 'delicious' in Japanese. MSG is known as a flavour enhancer because glutamate not only evokes a flavour but also enhances the existing flavours (Freeman, 2006). Especially the combination of MSG and table salt has been preferred (Ault, 2004). People consume glutamic acid in their daily nutrition in two ways: naturally through foodstuffs that contain glutamic acid and as a flavour enhancer (MSG) in food products. Commercial MSG is added to food products 'openly' (i.e. declared on labels) or without declaration on the labels. When MSG or other glutamic acid salts are added to food products, these salts dissociate in aqueous solutions and free glutamic acid is released (Beyreuther *et al.*, 2007). The most well-known MSG-added food products are meats, soups, bouillon cubes, sauces, dressings, chips, snacks, seasonings, meatballs and other ready-to-eat products (Skurray and Pucar, 1988). Previous studies have reported that the safety status of MSG has been contentious. While the US Food and Drug Administration has included it among the generally recognised as safe (GRAS), some scientific studies have associated the consumption of MSG with health problems (Lau and Mok, 1995).

In previous findings, MSG was identified as the cause of the so-called Chinese restaurant syndrome, which is typically associated with headache, burning sensations, facial pressure and chest pain (Schaumburg *et al.*, 1969). It was reported that MSG can trigger asthma and migraine (Freeman, 2006). Furthermore, associations between diabetes and obesity and MSG consumption have also been observed in both human and animal research studies (Shannon *et al.*, 2017). These findings demonstrate MSG as an endocrine disruptor food additive. According to the Turkish Food Codex (TFC) and European Union Directives (EC), the highest allowed MSG concentration is 10 g/kg.

Considering the research findings that have presented the unwanted impacts of MSG on health, the development and application of effective and robust methods for the determination of additional MSG in foodstuffs have necessitated a need for public concerns. Several studies were dedicated with the aim of detecting glutamic acid in foods. In general, chromatographic, spectrophotometric and fluorometric techniques were applied for the determination of glutamic acid and its salts (Acebal *et al.*, 2008). Populin *et al.* (2007) performed a survey study for the determination of free glutamic acid content of a variety of foods by using high-pressure liquid chromatography (HPLC) technique. Cebi *et al.* (2018) developed a liquid chromatography tandem-mass spectrometry (LC-MS/MS) chromatographic method for the determination of free glutamic acid content in chips, soups, sauces and dressings. Khampha *et al.* (2004) used a flow injection analysis system for the selective determination of L-glutamate in food samples, while Aung and Pyell (2015) determined the MSG in canned foods by using capillary electrophoresis. Importantly, MSG is added to the stock cubes at high amounts, and Demirhan *et al.* (2015) investigated the MSG levels of beef and chicken stock cubes in Ankara, Turkey, using HPLC technique. As seen, chromatographic techniques were used in most of the previous studies. The applied techniques are powerful and it is possible to obtain reliable results through these techniques. However, real-time monitoring and rapid detection systems are needed in order to detect adulterants in food control systems. Especially, precise and robust techniques are required for ensuring food safety, food quality and authenticity. Numerous non-destructive and effective techniques (e.g. Raman, Infrared, fluorescence, X-ray and electronic nose) have potential for overcoming the mentioned problems. Recent studies have shown that as an emerging technique, chemical or spectroscopic imaging combines conventional imaging and spectroscopy to gather spatial and spectral features from complex food matrix (Gowen *et al.*, 2007). When considered from a food chemistry point of view, food and agricultural products can be considered as a mixture of structural components. Recent evidence has reported that Raman spectroscopy has been applied to detect suspicious molecules in a complex food matrix. Analytes that are convenient for Raman analysis involve food's major components (e.g. proteins, fats and carbohydrates) and minor components (e.g. carotenoids and inorganics), as well as extrinsic components (e.g. bacteria and adulterants) (Qin *et al.*, 2014). Previous studies have reported that Raman spectroscopy was successfully applied in various challenging food safety problems. However, the main weakness of these studies was the lack of spatial information. Raman microscopy (chemical imaging or chemical mapping) systems provide spectral and spatial information about food surface and thus present high-throughput solutions for food safety and quality problems (Qin *et al.*, 2014). A number of studies have investigated the accomplishments of Raman imaging technique in food safety problems. Raman hyperspectral imaging was used for the detection of green pea adulteration in pistachio nut granules and green pea granules were determined at the concentration of 20–80% (Eksi-Kocak *et al.*, 2016). Qin *et al.* (2013) successfully determined multiple adulterants (e.g. ammonium sulphate, dicyandiamide, melamine and urea) in dry milk using macro-scale Raman chemical imaging. In another study, Qin *et al.* (2011) showed that lycopene changes in tomatoes could be successfully detected in order to track ripening using Raman imaging. Yongliang *et al.* (2009) accomplished the identification and imaging of melamine in wheat flour matrix using Raman chemical imaging technique.

This study was conducted with the aim of detecting additional MSG in dry soup mixtures using sensitive and specific Raman mapping techniques. The different aspects and novelties of our study are that, for the first time, we used Raman chemical mapping technique for the detection of MSG (four different types) in dry soup mixtures (prepared in a laboratory) and commercial dry soups (purchased from markets). In addition, the obtained results were confirmed using a robust LC-MS/MS method for commercial dry soups.

2. Materials and methods

Apparatus, reagents and materials

Measurements were gathered using Renishaw Raman microscope system, equipped with an Olympus 20× objective lens. Instrument control, data acquisition and mapping operations were performed by using Wire 3.4 (Renishaw, Gloucestershire, UK) software. A ball mill mixer (Retsch MM400, Haan, Germany) and hydraulic pellet press machine (Perkin Elmer, Norwalk, USA) were used for sample preparation before analysis. Raman spectra of ingredients in the composition of adulterated dry soup mix are presented in Figure 1. MSG (molecular formula: $C_5H_8NNaO_4$ was

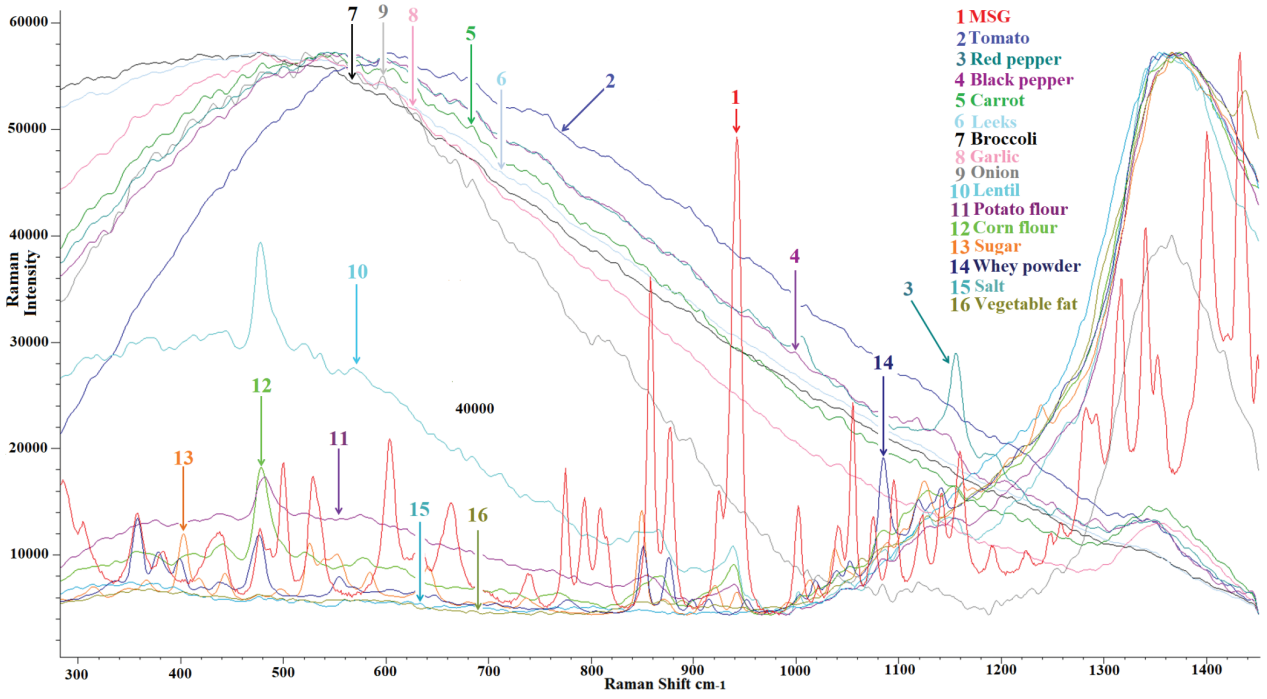

Figure 1. Raman spectra of ingredients in the composition of adulterated dry soup mix.

provided by Sigma Aldrich (Sigma-Aldrich GmbH, Sternheim, Germany). Two different types of standard MSG—L-glutamic acid monosodium salt hydrate (G1626) and L-glutamic acid monosodium salt monohydrate (49621)—were purchased from Sigma Aldrich. Additionally, two different types of commercial MSG were obtained from Alfasol and Tito (Turkey), which were coded as Brand A and Brand B, respectively. For the preparation of the dry soup mix, dried vegetables (e.g. carrot, broccoli, leeks and tomato), garlic and onion were purchased from Kurucum Gıda (Turkey). Lentil powder, salt, corn flour, sugar, red pepper and black pepper were purchased from a local supermarket (İstanbul, Turkey). Whey powder, potato flour and vegetable fat powder were obtained from Maybi (Turkey), Tito (Turkey) and As Gıda (Turkey), respectively. Four different types of commercial dry soup products were obtained from a local supermarket in İstanbul.

Sample preparation

Dry soup mix was prepared according to the study of Abeysinghe and Illeperuma (2006), with some modifications. The percentages of ingredients in the soup mix were determined as follows: dried vegetables (25%), tomato powder (7%), lentil powder (12%), potato flour (10%), corn flour (9%), whey powder (18%), salt (12%), sugar (2%), spice mix (1%) and vegetable fat (4%). Soup mix was enriched with four types of MSG (G1624, 49621, Alfasol and Tito) at percentages of 0.1, 0.2, 0.4 and 0.6%. All of the samples were mixed diligently using vibratory ball milling for 10 min in order to obtain a perfectly homogeneous mixture of dry soup mix and MSG.

Then pellets of adulterated soup samples were prepared by applying a pressure of 10 MPa for approximately 1 min in pellet press. Pellet preparation was performed without KBr; the aim of this operation was to obtain a perfectly smooth and plain sample surface before Raman microscopy analysis.

Analysis by LC-MS/MS

LC-MS/MS analyses were performed by using (Shimadzu UFLC LC-20AD) HPLC system (Shimadzu Corporation, Kyoto, Japan). EZ:FAAST (4 µ AAA-MS 250×2 mm) column was used. A gradient programme was applied for chromatographic separation (1 mmol/L formic acid in water: A; 1 mmol/L formic acid in water: B). The oven temperature was maintained at 40 °C with a flow rate of 0.25 ml/min. The gradient profile was scheduled as follows: 0.1 min, 38% B; 12 min, 65% B; 12.1 min, 95% B; 14 min, 95% B; 14.1 min, 38% B; and 20 min, 38% B. The injection volume was 10 µl. The LC-MS/MS system consisted of an HPLC (Shimadzu) coupled with Applied Biosystems MDS SCIEX 4000 Q TRAP mass spectrometer. The MS/MS detector

conditions were as follows: curtain gas 20 ml/min, exit potential 10 V, ion source gas 1 and ion source gas 2 were set at 50 ml/min, ion spray voltage was set at 5,500 V and turbo spray temperature was set at 550 °C. MS data were acquired in the positive ion electrospray ionization (ESI) mode using two alternating MS/MS scan events.

Raman measurements

Raman spectra of all samples were obtained by using Renishaw Raman microscope system, equipped with an Olympus 20X objective lens. Raman spectra were excited using 785-nm radiation from a diode array laser and 50% laser power applied to the sample with 0.1 s exposure time. A 1040×256 pixels Renishaw charge coupled device (CCD) camera was used in the experiment. Spectra were collected over the range of 281–1,451 cm^{-1}. To improve the signal-to-noise ratio of the data, 15 scans (accumulation) were preferred to obtain spectra and cosmic ray removal was used in all measurements.

Chemical mapping

Dry soup mix samples (~1 cm diameter) were placed on microscope slides that were mounted on the motorised xyz stage of the inVia Raman spectrometer (Renishaw Plc., Wotton-under-Edge, Gloucestershire, UK) equipped with confocal capability, a 785-nm diode laser (500 mW) and a 1,200 L/mm grating. The instrument wavelength was calibrated with silicon at 520 cm^{-1}. The instrument was operated using 20X objective lens, a 65-µm slit and a 1040×256 pixels Renishaw CCD camera. Each data set was analysed using the Renishaw WIRE 3.4 software. rectangle map type was selected at 1,500 µm ×1,500 µm area for mapping operation and the step was 75 in all measurements. Raw data were subjected to component analysis; thus, component maps were created using Wire 3.4 software. Standard MSG was selected as searched component, first derivative and normalisation was performed in the developed methodology.

LC-MS/MS analysis

LC-MS/MS analysis of commercial dry soup samples was performed according to the method described by Cebi *et al*. (2018). The method includes derivatisation steps. About 10 g of dry soup samples was mixed diligently using vibratory ball milling prior to the analysis. Subsequently, 20 ml of 0.1 N HCl was transferred onto the 50 mg of sample and the sample was kept in an ultrasonic water bath for 30 min. After filtration, derivatisation process was performed through four steps. Finally, the dried upper phase was dissolved in 1,000 µl of methanol/water (80:20) and the final solution was filtered through a 0.45-µm filter prior to LC-MS/MS analysis. The LC-MS/MS analysis of four different commercial dry soup samples was performed using this technique.

3. Results and discussion

Characterisation of Raman spectrum of MSG

MSG has very distinct, specific and obvious Raman bands with respect to other components in the dry soup mix. Raman spectra of MSG and all other soup ingredients are presented in Figure 1. Raman spectra of four different MSG and band assignment of MSG are shown in Figure 2. The obtained Raman spectra were identical for four types of MSG samples as shown in Figure 2. The spectrum had significant vibrational bands at 382, 441, 478, 500, 529, 603, 665, 740, 775, 792, 808, 858, 877, 925, 943, 1,003, 1,041, 1,056, 1,076, 1,097, 1,124, 1,142, 1,161, 1,193, 1,284, 1,293, 1,318, 1,342, 1,353, 1,402 and 1,434 cm^{-1}. These bands are within the scope of fingerprint region. These bands were associated with the chemical groups of components present in the chemical structure of MSG. The band with a peak point at 1,434 and 1,353 cm^{-1} corresponds to the CH_2 deformation and wagging modes (Shurvell and Bergin, 1989). The strong band at 1402 cm^{-1} is due to symmetrical COO^- stretching vibrations (Navarrete *et al.*, 1994). Vibrational bands at 1,318, 1,342, 1,293, 1,284, 1,193 and 1,161 cm^{-1} are responsible for the CH_2 deformation vibrations (i.e. twisting and wagging) (Peica *et al.*, 2007). The most characteristic band for carboxylic acid dimers 960–875 cm^{-1} is due to the in-plane and out-of-plane OH···O wagging modes (Kabischt and Klose, 1978). The band with a peak point at 1,124 cm^{-1} corresponds to the NH_2 twisting and NH_3^+ rocking modes (Dhamelincourt and Ramírez, 1991). The band at 1,097 cm^{-1} is due to the CH_2 rocking mode, while the medium band at 1,076 cm^{-1} corresponds to the NH_3^+ rocking mode and to the C–N stretching mode (Shurvell and Bergin, 1989). The band at 1,056 cm^{-1} and the weak peak at 1,041 cm^{-1} are resulted from the C–C stretching vibrations and CH_2 rocking mode, respectively (Navarrete *et al.*, 1994). Additionally, weak bands at 382, 441 and 478 cm^{-1} are mainly due to skeletal bending vibrations, (OH, CH) bending vibrations and NH_3^+ twisting vibrations, respectively (Peica *et al.*, 2007).

Importantly, the band at 500 cm^{-1} arises from COO^- rocking and $NH3^+$ torsion modes and the bands at 633 and 603 cm^{-1} are due to the COO^- scissoring and wagging modes, respectively (Dhamelincourt and Ramírez, 1991; Navarrete *et al.*, 1994; Peica *et al.*, 2007). The strong band at 665 cm^{-1} corresponds to the COOH in-plane bending vibrations (Navarrete *et al.*, 1994; Peica *et al.*, 2007). The peaks at 775 and 740 cm^{-1} are due to the COO^- bending vibrations of glutamic acid. The bands

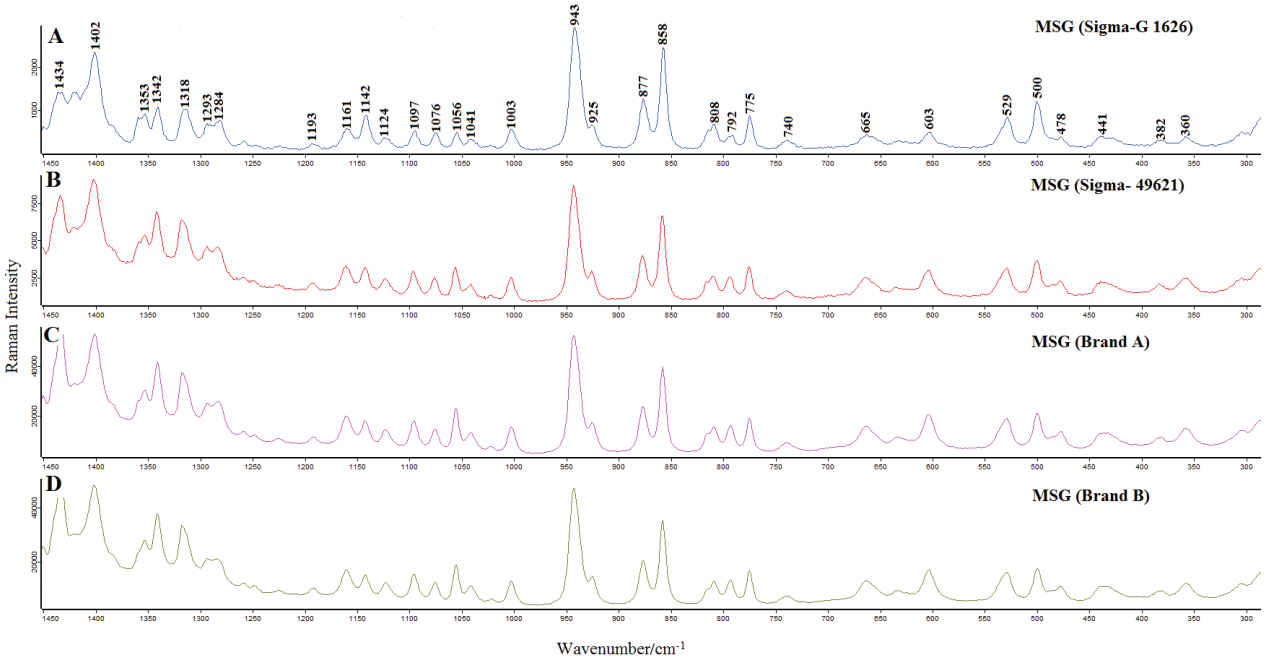

Figure 2. Raman spectra of monosodium glutamate from different brands: (A) Sigma-G1626, (B) Sigma-49621, (C) Brand A and (D) Brand B.

with a peak point at 792 and 808 cm^{-1} are responsible for the NH_2 bending vibrations and CO and N–H deformation vibrations, respectively (Peica *et al.*, 2007). Lastly, a strong band at 858 cm^{-1} corresponds to the COOH deformation vibrations and O–O stretching vibrations (Shurvell and Bergin, 1989).

Creating multivariate images

Preprocessing

During the application of a spectroscopic technique, preprocessing is a very important step in data analysis. While performing a mapping operation, data preprocessing is performed in order to assist the extraction of chemical information in subsequent data analysis procedure by reducing undesirable signals from particle size effects, morphological differences and detector artefacts (Zhang *et al.*, 2005). In this study, derivation (first order) and Savitzky–Golay normalisation were performed accompanied by direct classical least squares (DCLS) (Renishaw, Wire) analysis. The derivation process could be regarded as a solution to the ordinary problems, especially in multicomponent samples. Obtained derivative spectra present more specific and characteristic profile in comparison to the non-derivative spectra. For example, one of the unwanted effects in the spectroscopy is baseline shift, which could be attributed to the instrument conditions or sample handling factors. The first derivative spectrum overcomes baseline shifts and improves the accuracy as the first derivative of a constant absorbance offset has been zero (Ekrami *et al.*, 2010). Savitzky–Golay smoothing/derivation employs a polynomial smoothing window around a central point to calculate the derivative value for that point. In this popular method, numerical derivation is performed and a polynomial is fitted in a symmetric window on the raw data. This process is applied to all points in the spectra sequentially (Savitzky and Golay, 1964). Additionally, Savitzky–Golay pre-treatment is a widely used method and has the potential to efficiently dispose noises like baseline drift, tilt, reverse and so forth (Chen *et al.*, 2013).

DCLS component analysis

When collecting Raman data from complex systems (e.g. soup mix), or those containing many different spectra, it is often inconvenient and inappropriate to use univariate methods to accurately determine the location and proportion of specific chemical species. Multivariate data analysis is ideal to investigate such systems. In this study, we used DCLS component analysis to obtain component (MSG) images in the adulterated soup mixtures (DCLS, Renishaw Wire 3.4 component analysis method). The multivariate data analysis technique used in this method is DCLS fitting of the unknown data to a linear combination of specified component spectra [referred to as 'components (DCLS)' in the Wire 3.4 software].

This method is generally preferred when reference spectra are available for the suspected components and involve fitting the unknown data (collected during mapping) to a linear combination of the specified component spectra. When a match was found to occur between the standard and the collected spectra, a false colour was assigned and separate false colour images were created for each component (McAughtrie *et al.*, 2013). Each reference spectrum is used to create separate images with lookup table (LUT) values between 0 and 1. Values close to 1 indicate areas within the image most similar in shape to that of the reference spectrum. Also, these regions (suspected matter-rich) appear red and brightest colour in the diagram for rainbow and Ice LUT, respectively. The LUT control allows the user to see the way that the LUT relates colour to data values.

Raman chemical mapping of MSG adulterant in dry soup mix

The application of Raman mapping technique, with excitation at 785 nm, for the detection of MSG in dry soup mix has resulted in high effectiveness. Raman chemical map (Rainbow LUT), regional spectrum and the white light image are shown in Figure 3A–3C, respectively. Raman maps were obtained from smooth surfaces of pressed pellets. Raman mapping was performed in an area of 1,500 μm×1,500 μm. Actually, it is possible to select the mapping within the maximum area of 200 μm × 200 μm using live video window. However, in most conditions, Raman image is greater in size than the field of view of the white light image; therefore, it is needed to perform mapping experiments over large areas. Hence, it is necessary to perform a montage of white light images and by this way it is also easier to define the image area from the montage. The montage white light image and selected mapping area are presented in Figure 3C.

As shown in the figure, mapping was performed within the selected region (white light image). In this process, reference spectra were defined (DCLS, Wire 3.4). Lut diagram of the map image shows the intensity of MSG (defined component) on the basis of colour gradient. Red (Rainbow LUT) colour shows the richest regions for MSG. Spectrum from this region is shown on the right sight of the Raman map (Figure 3B). The presence of characteristic bands of MSG provided a good basis for selective Raman mapping to detect MSG adulteration or distribution in mixed dry soups. Characteristic bands of MSG were defined in previous sections. There are seven bands (500, 603, 665, 775, 793, 810 and 858 cm^{-1}) as specific for MSG because these bands were not observed in Raman spectra of other ingredients in the composition of dry soup mix. As shown in Figure 3B, the strongest MSG band at 858 cm^{-1} demonstrates the presence and distribution of this compound in the mix composition. Also MSG has distinct and specific spectral features with sharp and strong bands compared to other mix ingredients. In the DCLS method, the whole spectrum of MSG was defined and the presence of suspected compound in different samples was evaluated. While evaluating the spectrum from red regions (Figure 3B), one can conclude that the most significant and intense band is observed at 858 cm^{-1}. As mentioned previously, the strong band at 858 cm^{-1} is due to COOH deformation vibrations and O–O stretching vibrations of MSG. Two-dimensional chemical structure of MSG is shown in Figure 3D. Additionally, Raman chemical map of adulterated dry soup mix (0.09 %) is shown in Figure 3E, as it can been seen red region wasn't observed in Figure 3E since the detection limit was % 0.1 for developed Raman microscopy methodology. Furthermore, MSG can also be added to foods 'covertly' as yeast extracts. In this study, Raman spectrum of yeast extract was obtained under same experimental conditions and a quite different Raman spectrum was obtained without clear or sharp bands compared to standard MSG (Sigma). In other words, with distinct spectral features, MSG could be easily discriminated from yeast extract using Raman technique. As a result, MSG will be detected even it is covertly added as yeast extracts to the soup mix. A comparison of Raman spectra of MSG and yeast extract is presented in Figure S1 in the supplementary file.

Detection of adulterant particles in dry soup mix

Chemical maps of adulterated soup mix samples are presented in Figure 4. As shown in the figure, dry soup mix was adulterated with four different types of MSG (Sigma G1626, Sigma 49621, Brand A and Brand B) at different percentages (0.1, 0.2, 0.4 and 0.6%). The same image-processing and measurement conditions were applied to all 16 adulterated samples. Chemical mapping was completed in 35 min for each sample. Final map images in which adulterant distribution was observed using Rainbow LUT are presented in Figure 4A. According to the Rainbow LUT, the richest regions for MSG are shown in red colour and the poorest regions for MSG are observed in darkest colour in chemical map. Chemical maps provide a clear view of identification and spatial distribution of adulterants in the mixture composition (Qin *et al.*, 2013). Adulterant type was previously defined in the DCLS method and maps were created by this way; however, it is possible to observe adulterant-specific Raman bands by drawing spectrum from MSG-rich regions (red regions) in chemical maps (Figure 4B). Clearly, the spectral and spatial information from Raman maps indicates where the component is located. Additionally, four commercial dry soup samples were analysed by using the same Raman mapping technique under

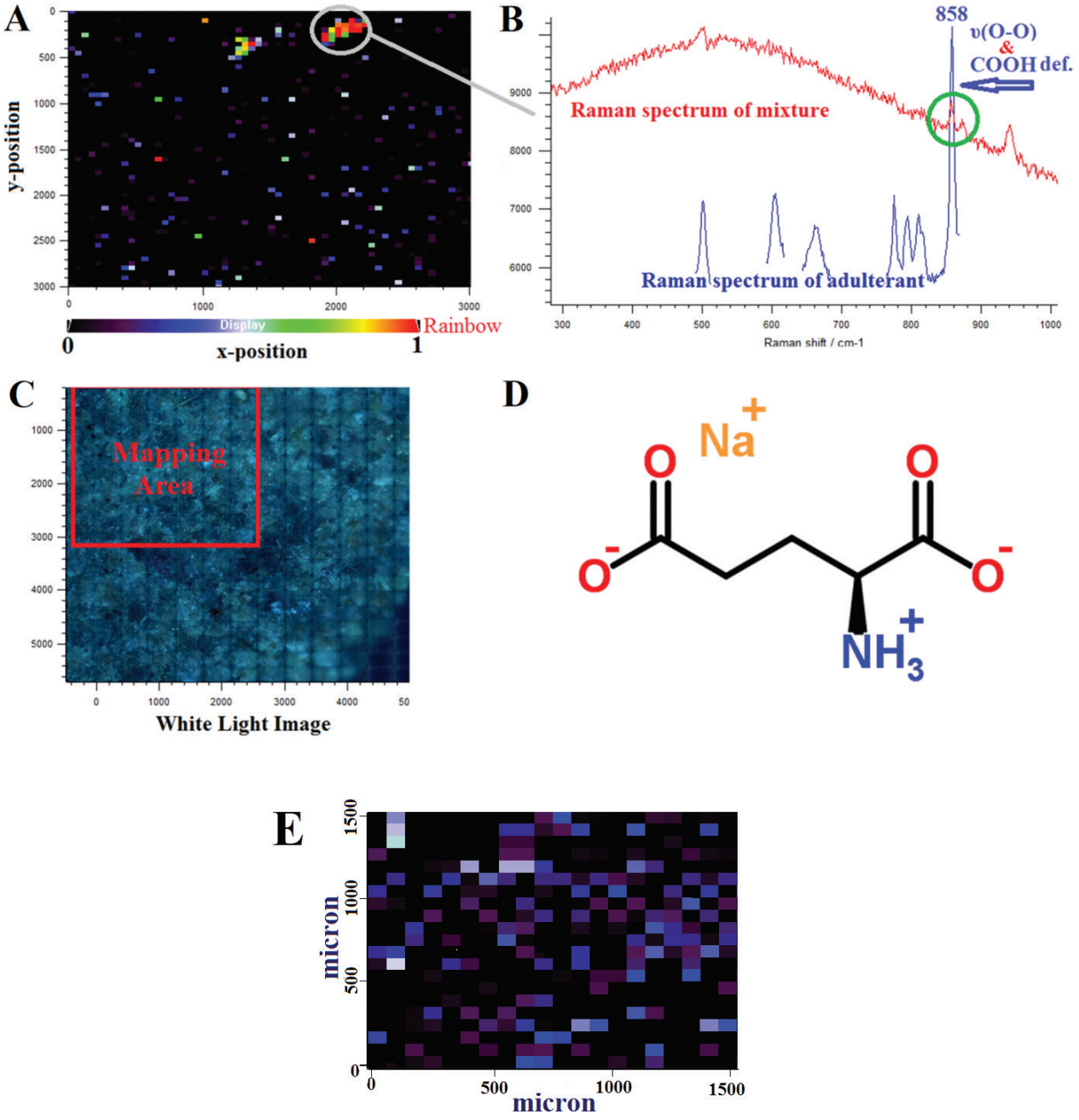

Figure 3. (A) Raman chemical map of adulterated dry soup mix (Rainbow lookup table). (B) Raman spectrum of monosodium glutamate (MSG)-rich region. (C) Montage white light image. (D) Two-dimensional chemical structure of MSG. (E) Raman chemical map of adulterated dry soup mix (0.09%).

same experimental conditions and MSG was detected in these samples too. Raman maps are presented in Figure 4B and the same spectral features were observed in MSG-rich regions of chemical maps. In commercial dry soup samples, the concentration of MSG is supposed to be at least 0.1% or above because detection limit of this method has been determined at 0.1%. LC-MS/MS analysis was performed for the determination of additional MSG content of commercial dry soup samples as described by Cebi *et al.* (2018). Reference LC-MS/MS method was performed with the aim of detecting additional MSG in foodstuff. MSG contents of dry soup samples were detected at 0.17, 0.34, 0.29 and 0.19 g/100 g for dry soup 1, dry soup 2, dry soup 3 and dry soup 4, respectively. Raman maps of these dry soup samples are presented in Figure 4B. Obviously, the LC-MS/MS results confirm Raman findings with regard to the presence of MSG in commercial dry soup samples.

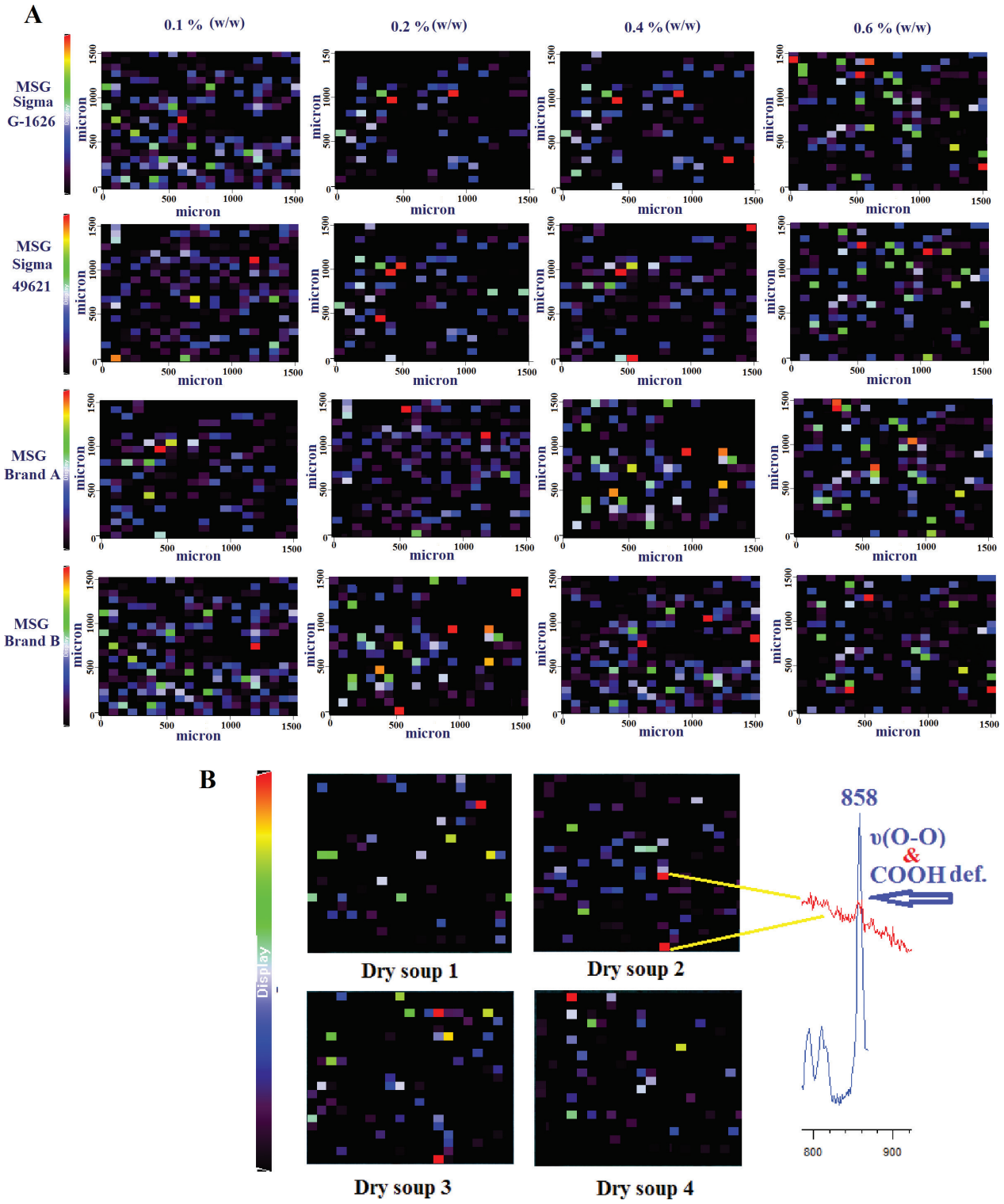

Figure 4. (A) Chemical maps of adulterated dry soup mix samples with monosodium glutamate (MSG) (Sigma G-1626), MSG (Sigma 49621), MSG (Brand A) and MSG (Brand B). (B) Chemical maps of commercial dry soup samples.

4. Conclusion

Rapid, accurate, non-destructive and effective authentication of food ingredients with minimal sample preparation is quite important in terms of food safety and quality. Our study developed, for the first time, the detection of MSG in dry soup mix using Raman mapping technique. Raman chemical maps can be obtained in only 35 min, and thus the detection of MSG in complex mixture composition. In this study, spectral and spatial distribution of MSG in complex soup composition (15 ingredients) was successfully accomplished using chemical mapping through DCLS (Renishaw, Wire 3.4) method. Raman mapping system is capable of acquiring sufficient spectral and spatial information to identify and map the adulterant particles mixed into the dry soup mixture.

One of the strengths of this study is that Raman maps perfectly show adulterants when the MSG adulteration is implemented at percentages of 0.1–0.6% (w/w) in dry soup mixture. In other words, MSG adulteration was determined with a detection limit of 0.1%. Finally, it can be concluded that the developed Raman microscopy technique is cost-effective, rapid, easy to operate, non-destructive and can be labelled as a 'green analytical technique' as no solvents and reagents were used during this study. In future studies, Raman chemical mapping holds promise for solutions to the challenging food adulteration, food safety and authentication issues.

Acknowledgements

This research is supported by the Project No. 115O065 of TUBITAK TOVAG 1003.

Conflict of interest

The authors declare no conflicts of interest with respect to the research, authorship and/or publication of this article.

Funding

This project was supported by TUBITAK with a project. We presented it in the acknowledgements. This project was financially supported by TUBITAK.

Compliance with ethical standards

This article followed all ethical standards for a research without direct contact with human or animal subjects.

References

Abeysinghe, C.P. and Illeperuma, C.K., 2006. Formulation of an MSG (Monosodium Glutamate) free instant vegetable soup mix. Journal of the National Science Foundation of Sri Lanka 34: 91–95. https://doi.org/10.4038/jnsfsr.v34i2.2087

Acebal, C.C., Lista, A.G. and Fernández Band, B.S., 2008. Simultaneous determination of flavor enhancers in stock cube samples by using spectrophotometric data and multivariate calibration. Food Chemistry 106: 811–815. https://doi.org/10.1016/j.foodchem.2007.06.009

Ault, A., 2004. The monosodium glutamate story: the commercial production of msg and other amino acids. Journal of Chemical Education 81: 347. https://doi.org/10.1021/ed081p347

Aung, H.P. and Pyell, U., 2015. In-capillary derivatization with o-phthalaldehyde in the presence of 3-mercaptopropionic acid for the simultaneous determination of monosodium glutamate, benzoic acid, and sorbic acid in food samples via capillary electrophoresis with ultraviolet detectio. Journal of Chromatography A 1449: 156–165. https://doi.org/10.1016/j.chroma.2016.04.033

Beyreuther, K., Biesalski, H.K., Fernstrom, J.D., Grimm, P., Hammes, W.P., Heinemann, U., Kempski, O., Stehle, P., Steinhart, H. and Walker, R., 2007. Consensus meeting: monosodium glutamate—an update. European Journal of Clinical Nutrition 61: 304–313. https://doi.org/10.1038/sj.ejcn.1602526

Cebi, N., Dogan, C.E., Olgun, E.O. and Sagdic, O., 2018. A survey of free glutamic acid in foods using a robust LC–MS/MS method. Food Chemistry 248: 8–13. https://doi.org/10.1016/j.foodchem.2017.12.033

Chen, H., Song, Q., Tang, G., Feng, Q. and Lin, L., 2013. The combined optimization of Savitzky-Golay smoothing and multiplicative scatter correction for FT-NIR PLS models. International Scholarly Research Notices 2013: 642190. https://doi.org/10.1155/2013/642190

Demirhan, B.E., Demirhan, B., Sönmez, C., Torul, H., Tamer, U. and Yentür, G., 2015. Monosodium glutamate in chicken and beef stock cubes using high-performance liquid chromatography. Food Additives & Contaminants: Part B 8: 63–66. https://doi.org/10.1080/19393210.2014.991355

Dhamelincourt, P. and Ramírez, F.J., 1991. Polarized micro-Raman and Fourier transform infrared spectra of L-glutamic acid. Journal of Raman Spectroscopy 22: 577–582. https://doi.org/10.1002/jrs.1250221007

Ekrami, E., Okazi, M., Kang, Q., Zhou, W., Li, Q., Gao, B., Fan, J., Shen, D., Turabik, M., Rojas, F.S., Ojeda, C.B., Pavon, J.M., Lettre, D.P., Patel, K.N., Patel, J.K., Rajput, G.C., Rajgor, N.B., Sahel, K., Perol, N., Dappozze, F., Bouhent, M., Derriche, Z. and Guillard, C., 2010. Analysis of dye concentrations using derivative spectrophotometric techniques. Talanta 212: 139–150.

Eksi-Kocak, H., Mentes-Yilmaz, O. and Boyaci, I.H., 2016. Detection of green pea adulteration in pistachio nut granules by using Raman hyperspectral imaging. European Food Research and Technology 242: 271–277. https://doi.org/10.1007/s00217-015-2538-3

Freeman, M., 2006. Reconsidering the effects of monosodium glutamate: a literature review. Journal of the

American Academy of Nurse Practitioners 18: 482–486. https://doi.org/10.1111/j.1745-7599.2006.00160.x

Gowen, A.A., O'Donnell, C.P., Cullen, P.J., Downey, G. and Frias, J.M., 2007. Hyperspectral imaging—an emerging process analytical tool for food quality and safety control. Trends in Food Science and Technology 18: 590–598. https://doi.org/10.1016/j.tifs.2007.06.001

Kabischt, G. and Klose, M., 1978. A Raman spectroscopic study of aqueous and methanolic tetrame thylammonium chloride solutions. Journal of Raman Spectroscopy 7: 311–315. https://doi.org/10.1002/jrs.1250070604

Khampha, W., Yakovleva, J., Isarangkul, D., Wiyakrutta, S., Meevootisom, V. and Emnéus, J., 2004. Specific detection of L-glutamate in food using flow-injection analysis and enzymatic recycling of substrate. Analytica Chimica Acta 518: 127–135. https://doi.org/10.1016/j.aca.2004.05.048

Lau, O.W. and Mok, C.S., 1995. Indirect conductometric detection of amino acids after liquid chromatographic separation. Part II. determination of monosodium glutamate in foods. Analytica Chimica Acta 302: 45–52. https://doi.org/10.1016/0003-2670(94)00423-J

McAughtrie, S., Lau, K., Faulds, K. and Graham, D., 2013. 3D optical imaging of multiple SERS nanotags in cells. Chemical Science 4: 3566. https://doi.org/10.1039/c3sc51437d

Navarrete, J.T.L., Hernandez, V. and Ramirez, F., 1994. Vibrational spectra of [15 N] glutamic acid and [2H4]glutamic acid. Journal of Raman Spectroscopy 25: 861–867. https://doi.org/10.1002/jrs.1250251104

Peica, N., Lehene, C., Leopold, N., Schlücker, S. and Kiefer, W., 2007. Monosodium glutamate in its anhydrous and monohydrate form: differentiation by Raman spectroscopies and density functional calculations. Spectrochimica Acta—Part A: Molecular and Biomolecular Spectroscopy 66: 604–615. https://doi.org/10.1016/j.saa.2006.03.037

Populin, T., Moret, S., Truant, S. and Conte, L.S., 2007. A survey on the presence of free glutamic acid in foodstuffs, with and without added monosodium glutamate. Food Chemistry 104: 1712–1717. https://doi.org/10.1016/j.foodchem.2007.03.034

Qin, J., Chao, K., Cho, B.K., Peng, Y. and Kim, M.S., 2014. High-throughput Raman chemical imaging for rapid evaluation of food safety and quality. Transactions of the ASABE 57: 1783–1792. https://doi.org/10.13031/trans.57.10862

Qin, J., Chao, K. and Kim, M.S., 2011. Investigation of Raman chemical imaging for detection of lycopene changes in tomatoes during postharvest ripening. Journal of Food Engineering 107: 277–288. https://doi.org/10.1016/j.jfoodeng.2011.07.021

Qin, J., Chao, K. and Kim, M.S., 2013. Simultaneous detection of multiple adulterants in dry milk using macro-scale Raman chemical imaging. Food Chemistry 138: 998–1007. https://doi.org/10.1016/j.foodchem.2012.10.115

Savitzky, A. and Golay, M.J.E., 1964. Smoothing and differentiation of data by simplified least squares procedures. Analytical Chemistry 36: 1627–1639. https://doi.org/10.1021/ac60214a047

Schaumburg, H.H., Byck, R., Gerstl, R. and Mashman, J.H., 1969. Monosodium L-glutamate: its pharmacology and role in the Chinese restaurant syndrome. Science (New York, N.Y.) 163: 826–828. https://doi.org/10.1126/science.163.3869.826

Shannon, M., Green, B., Willars, G., Wilson, J., Matthews, N., Lamb, J., Gillespie, A. and Connolly, L., 2017. The endocrine disrupting potential of monosodium glutamate (MSG) on secretion of the glucagon-like peptide-1 (GLP-1) gut hormone and GLP-1 receptor interaction. Toxicology Letters 265: 97–105. https://doi.org/10.1016/j.toxlet.2016.11.015

Shurvell, H.F. and Bergin, F.J., 1989. Raman spectra of L(+)-glutamic acid and related compounds. Journal of Raman Spectroscopy 20: 163–168. https://doi.org/10.1002/jrs.1250200307

Skurray, G.R. and Pucar, N., 1988. L-Glutamic scid content of fresh and processed foods. Food Chemistry 27: 177–180. https://doi.org/10.1016/0308-8146(88)90060-X

Yongliang, L., Chao, K., Kim, M.S., Tuschel, D., Olkhovyk, O. and Priore, R.J., 2009. Potential of Raman spectroscopy and imaging methods for rapid and routine screening of the presence of melamine in animal feed and foods. Applied Spectroscopy 63: 477–480. https://doi.org/10.1366/000370209787944398

Zhang, L., Henson, M.J. and Sekulic, S.S., 2005. Multivariate data analysis for Raman imaging of a model pharmaceutical tablet. Analytica Chimica Acta 545: 262–278. https://doi.org/10.1016/j.aca.2005.04.080